Derna Academy Journal for Applied Sciences

E-ISSN: 3006-3159

DAJAS

Morphological Characterization and *rbcL* DNA Barcoding of Wild *Sonchus oleraceus* from Omar Al-Mukhtar University Campus, Al-Bayda, Libya

Latifa S. El-Saifat [1], Zakia Kh. Idris [2*], Ahmed Mahmoud Ismail [3]

[1,2] Department of Forestry, Faculty of Natural Resources and Environmental Science, Omar Al-Mukhtar University, Al-Bayda, Libya

[3] Pests and Plant Diseases Unit, College of Agricultural and Food Sciences, King Faisal University, Al-Ahsa 31982, Saudi Arabia

التوصيف المورفولوجي والترميز الشريطي لجين *rbcL* في نبات الجعضيض البري (*Sonchus oleraceus*) من حرم جامعة عمر المختار، البيضاء، ليبيا

لطيفة سليمان الصيفاط [1]، زكية خليفة ادريس[2*]، أحمد محمود إسماعيل[3]

[1, 2] قسم الغابات، كلية الموارد الطبيعية وعلوم البيئة، جامعة عمر المختار، البيضاء، ليبيا

[3] وحدة آفات النبات وأمراضه، كلية العلوم الزراعية والأغذية، جامعة الملك فيصل، الأحساء 31982، المملكة العربية السعودية

*Corresponding author: E-mail address: zakiah.idris@omu.edu.ly

Volume: 8 | **Issue: 1** | **Page Number: 95 - 114**

Keywords: Sonchus oleraceus; rbcL barcoding; phenotypic variability; biomass allocation trade-off; morphology–molecular concordance

Copyright: © 2026 by the authors. Licensee: The Derna Academy for Applied Science (DAJAS). This article is an open access article distributed under the terms and conditions of the Creative Commons Attribution (CC BY) License (https://creativecommons.org/licenses/by/4.0/)

Received: 01\10\2026
Accepted: 12\10\2026
Published: 13\10\2026

https://doi.org/10.71147/9hv3ty75

ABSTRACT

This study integrates morphometric characterization with *rbcL* DNA barcoding to document wild *Sonchus oleraceus* L. from the Omar Al-Mukhtar University campus, Al-Bayda, Libya. Thirty individuals were sampled from six microhabitats, and ten vegetative, reproductive, and biomass traits were analyzed using descriptive statistics, Pearson correlation, and regression. Vegetative and biomass traits were highly variable (shoot fresh weight coefficient of variation, CV = 78.9%), whereas inflorescence length was comparatively uniform (CV = 17.5%). Plant height and root length were strongly correlated (r = 0.942; within-microhabitat r = 0.90), and inflorescence count was inversely related to shoot dry weight (p = 0.002, R^2 = 28.89%), consistent with a resource-allocation trade-off that remained robust to multiple-testing correction and microhabitat clustering. Voucher examination confirmed that diagnostic characters matched the circumscription of *S. oleraceus*. For independent verification, genomic DNA was extracted from a pooled sample of the same population, and a partial *rbcL* region was amplified, sequenced, and analyzed against 25 reference Asteraceae sequences from GenBank. Maximum-likelihood analysis placed the accession within a strongly supported *S. oleraceus* clade (bootstrap = 98%), sister to *S. arvensis* (bootstrap = 96%), separating *Sonchus* from all other genera. Morphological and molecular evidence were concordant. Because the molecular analysis relied on a single pooled accession, the results confirm species-level identity but do not characterize intraspecific genetic diversity; they nonetheless provide a first reference *rbcL* sequence for *S. oleraceus* from Libya, addressing the near-absence of North African accessions in public databases.

الملخص :

تدمج هذه الدراسة بين التوصيف المورفومتري والترميز الشريطي للحمض النووي (DNA barcoding) باستخدام جين *rbcL* لتوثيق نبات الجعضيض البري *Sonchus oleraceus*.L من حرم جامعة عمر المختار، البيضاء، ليبيا. جُمعت ثلاثون عينة نباتية من ست بيئات دقيقة (microhabitats)، وحُلّلت عشر صفات خضرية وتكاثرية وصفات للكتلة الحيوية باستخدام الإحصاء الوصفي ومعامل ارتباط بيرسون والانحدار. أظهرت الصفات الخضرية وصفات الكتلة الحيوية تبايناً مرتفعاً (بلغ معامل الاختلاف للوزن الطازج للمجموع الخضري 78.9%)، في حين كان طول النورة متجانساً نسبياً (معامل الاختلاف 17.5%). وارتبط ارتفاع النبات بطول الجذر ارتباطاً قوياً (r = 0.942؛ وr داخل البيئات الدقيقة = 0.90)، وارتبط عدد النورات عكسياً بالوزن الجاف للمجموع الخضري (R^2 = 28.89%، p = 0.002)، بما يتسق مع مفاضلة في توزيع الموارد ظلّت متماسكة بعد تصحيح المقارنات المتعددة وبعد مراعاة التجمّع ضمن البيئات الدقيقة. وأكد فحص العينات المرجعية (voucher) أن الصفات التشخيصية تتطابق مع وصف النوع *S. oleraceus*. وللتحقق المستقل، استُخلص الحمض النووي الجينومي من عينة مجمّعة من المجتمع النباتي نفسه، وجرى تضخيم منطقة جزئية من جين *rbcL* وتسلسلها وتحليلها مقارنةً بـ 25 تسلسلاً مرجعياً لنباتات من الفصيلة المركّبة (Asteraceae) من بنك الجينات GenBank. وضع تحليل الأرجحية العظمى (Maximum Likelihood) العيّنة ضمن فرع قوي الدعم للنوع *S. oleraceus* (قيمة الإقلاع bootstrap = 98%)، شقيقاً للنوع *S. arvensis* (bootstrap = 96%)، وفاصلاً جنس *Sonchus* عن بقية الأجناس. وكان الدليلان المورفولوجي والجزيئي متوافقين،ولأن التحليل الجزيئي اعتمد على عينة واحدة مجمّعة، فإن النتائج تؤكد هوية النوع ولا تصف التنوع الوراثي داخل النوع؛ ومع ذلك فهي توفّر أول تسلسل مرجعي لجين *rbcL* للنوع *S. oleraceus* من ليبيا، ما يسدّ جزءاً من النقص الشديد في التسلسلات الشمال أفريقية في قواعد البيانات العامة.

الكلمات المفتاحية: *Sonchus oleraceus*؛ الترميز الشريطي لجين *rbcL*؛ التباين المظهري؛ المفاضلة في توزيع الكتلة الحيوية؛ التوافق المورفولوجي–الجزيئي

1. INTRODUCTION

Wild plants are fundamental components of terrestrial ecosystems, supporting biodiversity conservation, soil stabilization, and ecosystem services, particularly in Mediterranean and semi-arid biomes where pronounced environmental gradients shape species distribution and phenotypic performance (Maestre et al., 2012). Asteraceae, one of the largest angiosperm families (~32,000 species), includes the genus *Sonchus* L., ruderal herbs that readily colonize disturbed habitats worldwide (Mandel et al., 2019). *S. oleraceus* L. (Asteraceae, tribe Cichorieae), commonly known as common sowthistle, was formally described by Linnaeus in 1753 and belongs to a genus comprising an estimated 60–100 annual, biennial, and perennial species (Kim, Kim, Cho, Kim, & Kim, 2020; Puri, Khandagale & Ansari, 2018; Ruiz-Rocamora, Obón, Ríos, Alcaraz, & Rivera, 2025). *S. oleraceus* is a cosmopolitan, erect annual to short-lived biennial herb, typically 20–150 cm tall, arising from a short taproot, with a hollow, longitudinally ridged stem exuding milky latex when damaged (Hutchinson, Colosi, & Lewin, 1984). Its native range is generally placed in the Mediterranean basin, North Africa, and western Asia, from where it has become naturalized across nearly all ice-free regions of the world (Hutchinson et al., 1984; Ruiz-Rocamora et al., 2025). Leaves are heteromorphic and pinnatifid, clasping the stem with sagittate auricles; capitula bear numerous bright yellow ligulate florets, and the fruit is a ribbed, unwinged cypsela topped with a wind-dispersed pappus (Puri et al., 2018; Sadeq & Aliwy, 2019). Reliable identification relies on a combination of vegetative and reproductive characters rather than any single trait (Kim et al., 2020). Relative to its close congener *S. asper*, *S. oleraceus* is distinguished chiefly by flatter, more deeply pinnatifid leaves with sharply acute auricles and by narrower, unwinged, transversely rugulose achenes, whereas *S. asper* has broader, smoother, occasionally winged achenes and rounded, tightly clasping auricles (Hutchinson et al., 1984). Pollen micromorphology offers a further diagnostic line of evidence (Sadeq & Aliwy, 2019). Cytogenetically, *S. oleraceus* is a putative amphidiploid (2n = 32) derived from hybridization between *S. asper* (2n = 18) and *S. tenerrimus* (2n = 14) (Cho, Kim, Kim, Mejías, & Kim, 2019; Hutchinson et al., 1984). Its chloroplast genome has been fully sequenced, confirming close phylogenetic affinity with *S. asper*, although the precise parentage of the hybrid origin remains unresolved (Cho et al., 2019). Seventeen nuclear microsatellite markers have since been developed for the species, supporting genetic-diversity and population-structure studies (Kim et al., 2020), and random amplified polymorphic DNA (RAPD) analysis has revealed genetically distinct population clusters associated with geographic distance in India, with direct relevance for weed management given documented herbicide resistance in Australian populations (Kaundal, Sharma, & Kulshrestha, 2021). The tender shoots and leaves of *S. oleraceus* are widely consumed as a wild leafy vegetable and valued for their high vitamin C, protein, and dietary-fibre content (Botella et al., 2024; de Paula Filho, Barreira, & Pinheiro-Sant'Ana, 2022; Guil-Guerrero, Giménez-Giménez, Rodríguez-García, & Torija-Isasa, 1998).

The species also has a long-standing history in North African traditional medicine, including in the Al-Jabal Al-Akhdar region, where it continues to be harvested as both food and folk remedy (Al-Traboulsi & Alaib, 2021), underscoring the importance of accurate morphological identification of wild material intended for such uses. Al-Jabal Al-Akhdar is one of Libya's most biologically diverse landscapes, where a Mediterranean climate and heterogeneous topography generate a mosaic of microhabitats expected to drive pronounced morphological variation in local *S. oleraceus* populations (Abd El-Ghani & Al Borki, 2024). Classical morphological identification alone, however, is increasingly insufficient for resolving taxonomic boundaries in ecologically plastic, taxonomically complex genera such as *Sonchus*, where macroscopic characters are strongly shaped by environmental conditions and ontogenetic stage (Kim, Lee, & Mejías, 2007). DNA barcoding has emerged as a robust, reproducible complement to morphology-based identification (Hebert, Cywinska, Ball, & deWaard, 2003; Hollingsworth, Graham, & Little, 2011), with the plastid loci rbcL (ribulose-1,5-bisphosphate carboxylase/oxygenase large subunit) and matK (maturase K) formally adopted by the Consortium for the Barcode of Life as the core land-plant barcode (CBOL Plant Working Group, 2009); given its well-documented resolving power within Asteraceae, rbcL was adopted here as the primary confirmatory barcode, deployed alongside classical morphometrics. Despite a growing ethnopharmacological literature, molecular characterization of *S. oleraceus* remains geographically skewed away from its presumed Mediterranean/North African centre of origin: existing microsatellite markers, chloroplast genome assemblies, and the most extensive population-genomic dataset to date were developed primarily from Korean, Spanish, and Australian accessions, the latter framed around reconstructing the species' invasion history rather than characterizing native North African diversity (Cho et al., 2019; Encinas-Viso, Morin, Raghu, & Broadhurst, 2022; Kim et al., 2020). Dedicated molecular surveys from Libya, Algeria, Tunisia, and Egypt remain conspicuously scarce in GenBank and BOLD Systems, hindering biodiversity inventories and conservation prioritization (Nithaniyal, Asir, & Sarkar, 2025). To our knowledge, no prior study has molecularly characterized *S. oleraceus* from Libya using the *rbcL* barcode marker. Accordingly, the present study was designed to pursue two complementary aims. First, it sought to conduct a detailed morphometric and biomass-based characterization of *S. oleraceus* individuals collected from representative microhabitats on the Omar Al-Mukhtar University campus, Al-Bayda (Al-Jabal Al-Akhdar region), Libya, establishing a voucher-based morphological framework documenting the diagnostic vegetative and reproductive traits of the species. Second, it sought to confirm the taxonomic identity of the same Libyan population through DNA barcoding of the plastid *rbcL* marker and to evaluate its discriminatory efficiency relative to closely related Asteraceae taxa, hypothesizing that the sampled accession would cluster phylogenetically with Mediterranean and other reference *S. oleraceus* accessions deposited in GenBank. By quantifying the pattern of trait variability across vegetative, biomass, and reproductive descriptors and by anchoring this morphological dataset to an independent molecular line of evidence, this integrated study provides a reproducible morphology–molecule baseline for the accurate identification, biodiversity documentation, and future ecophysiological, taxonomic, and conservation-oriented research on *S. oleraceus* and other under-investigated wild Asteraceae taxa in North African Mediterranean ecosystems.

2. METHOD

2.1 Study Site and Plant Material

A descriptive morphological study was conducted on the main campus of Omar Al-Mukhtar University, Al-Bayda, Libya (Latitude: 32°45′30″ N, Longitude: 21°42′44″ E), a locality situated within the broader Al-Jabal Al-Akhdar region. Sampling was carried out during the flowering season in May 2025. The target species was the annual sowthistle (*S. oleraceus* L., Asteraceae), a locally prominent wild herb. A total of 30 healthy, uniform individuals were randomly selected from six distinct ecological microhabitats distributed across the university campus, with five plants harvested per site ($n = 5 \times 6 = 30$). This sampling design was intentionally confined to a single, well-defined campus locality and should accordingly be interpreted as a site-level case study rather than a survey representative of the wider Al-Jabal Al-Akhdar landscape. All specimens were collected concurrently at the full anthesis (flowering) stage to ensure developmental uniformity across sites (Boulos, 2000; Hutchinson et al., 1984), within the same growing season and under comparable environmental conditions to minimize confounding environmental variability. This same population subsequently served as the source material for the molecular confirmation analyses described in Section 2.5.

2.2 Morphological and Biomass Measurements

Immediately following collection, the botanical samples were transferred to the laboratory for processing and morphometric assessment. The standard protocol for phenotypic characterization included the tracking of both vegetative and reproductive traits. Vegetative attributes comprising plant height (cm), root length (cm), and leaf length (cm) were recorded using a standardized metric tape and a precision laboratory ruler. Quantitative variables, specifically the total number of leaves and inflorescences per plant, were manually counted, while inflorescence length was determined using a digital caliper and measured in cm.

For biomass determination, the harvested plants were meticulously cleaned with distilled water to remove adhering soil particles and debris, and then gently blotted dry. The fresh weight (g) of each plant was recorded immediately using an analytical digital balance (precision 0.001 g). Subsequently, to ascertain the dry matter accumulation, the samples were subjected to thermal dehydration. The plants were placed in a laboratory hot-air oven at 70°C until a constant dry weight (g) was achieved.

Representative fresh and pressed voucher material was additionally retained and photographed against linear scales including, for the isolated achene, a microscope-slide micrometer scale graduated in 0.1 mm intervals rather than a standard millimetre ruler, to document the diagnostic vegetative and reproductive characters of the sampled individuals.

2.3 Photographic Documentation and Climatic Data Acquisition

High-resolution digital photographs of the voucher specimens were captured directly by the authors under standardized lighting conditions to ensure consistent reproduction of diagnostic morphological detail. Post-capture image adjustments were strictly limited to global brightness and contrast optimization and to cropping for the removal of background artefacts, all performed using Photopea image-editing software. No non-linear enhancements, selective object manipulation, or generative artificial intelligence (AI) tools were applied to any of the images presented in this study.

Solar radiation and meteorological data underlying the climatic context reported in Section 5.2 were obtained from the National Aeronautics and Space Administration Prediction of Worldwide Energy Resources (POWER) Data Access Viewer (National Aeronautics and Space Administration [NASA], n.d.), for the geographical coordinates of the study site (Latitude: 32°45′30″ N, Longitude: 21°42′44″ E). Monthly precipitation for 2023–2025 (Supplementary Table S1) was retrieved, and cumulative January–May totals were used to characterize the three-year rainfall trend discussed in Section 5.2, whereas monthly air temperature and relative humidity records for 2024–2025 (Supplementary Table S2) were retrieved for the interannual (2024 vs. 2025) thermal and humidity comparisons presented in that section.

2.4 Statistical Analysis

Morphometric and biomass data were statistically analyzed using Minitab software (Version 21, Minitab Inc.) and Python (v3.12; SciPy and statsmodels libraries). Descriptive statistics were first applied to summarize the baseline characteristics of the variables; quantitative data were expressed as the mean ($\bar{x}$) to measure central tendency and the standard deviation (SD) to evaluate data dispersion. Second, Pearson's correlation coefficient (r) was calculated to evaluate the strength and direction of relationships between continuous variables; because the full correlation matrix comprised 45 simultaneous pairwise comparisons, exact two-tailed p-values were additionally computed for every pair and subjected to Benjamini–Hochberg false-discovery-rate (FDR) correction at $q = 0.05$ to control the family-wise Type I error rate. Third, linear regression analysis was performed to model the relationship between selected independent and dependent variables and to assess the predictive value of each model; residuals of all fitted models were evaluated for normality (Shapiro Wilk test) and homoscedasticity (Breusch–Pagan test), and Cook's distance was used to flag influential observations. Fourth, because the 30 sampled individuals were drawn in balanced blocks of five plants from each of six microhabitats, the potential for non-independence (pseudoreplication) arising from this nested design was explicitly evaluated: the intraclass correlation coefficient (ICC) attributable to microhabitat was estimated for each trait using random-intercept mixed-effects models, and correlations or regressions involving traits with non-negligible microhabitat clustering ($ICC > 0.10$) were re-evaluated as within-site partial correlations (residualized on microhabitat) and, for the principal regression model, using cluster-robust standard errors and a random-intercept mixed-effects model with microhabitat as the clustering unit. Statistical significance was set at $p \leq 0.05$ unless otherwise noted.

2.5 DNA Extraction

After completion of all morphological measurements on the sampled population, healthy leaf tissues were collected from the sampled plants and pooled to obtain a single representative composite sample of the studied population, since the molecular analysis was performed exclusively to confirm taxonomic identity and was not intended to assess intraspecific genetic variation or population genetic diversity. Genomic DNA was extracted from 10 to 30 mg of the pooled leaf material using the cetyltrimethylammonium bromide (CTAB) method (Doyle & Doyle, 1987). The quality and concentration of the DNA extract were determined using a NanoDrop spectrophotometer (Thermo Fisher Scientific, MA, USA).

2.6 PCR Amplification

Polymerase chain reaction (PCR) amplification of part of the ribulose-1,5-bisphosphate carboxylase/oxygenase large subunit (*rbcL*) gene region was performed using the universal primers rbcL-BF (5′-ATGTCACCACAAACAGAAAC-3′) and rbcL-724R (5′-TCGCATGTACCTGCAGTAGC-3′) (Wattoo et al., 2016). The PCR reaction was carried out in a 25 µL reaction volume, containing 10 µL PCR Master Mix (amaR OnePCR, GeneDirex, Inc.), 11 µL of ddH_2O, 1.5 µL of each primer, and 1 µL of template DNA. PCR was conducted in a 2720 Thermal Cycler (Applied Biosystems, Foster City, California). PCR amplification conditions, as indicated by Alshehri et al. (2019), included the following steps: an initial denaturation step at 94°C for 5 min, followed by 35 cycles of denaturation (94°C for 30 sec), annealing (50°C for 30 sec), and elongation (72°C for 30 sec), and ending with a final elongation step at 72°C for 7 min.

PCR products were separated on 1% (w/v) agarose gels (BIOMATIK™, Kitchener, Ontario, Canada) in 1× Tris-Acetate-EDTA (TAE) buffer. To visualize the DNA, 5 µL of diluted ethidium bromide (Sigma-Aldrich, St. Louis, USA) was added to the agarose gel before solidification. PCR products were loaded onto the gel using DNA loading buffer (BIOMATIK™, Kitchener, Ontario, Canada). The size of the PCR amplicons was determined using a 1000 bp DNA ladder (Promega, Madison, WI, USA).

2.7 DNA Sequencing

The amplified *rbcL* fragments were sequenced in both directions using the same primer pair employed for amplification. The PCR products were purified and sequenced via the Macrogen Inc. sequencing service (Seoul, South Korea). Sequencing reactions were performed using the BigDye Terminator Sequencing Kit v.3.1 (Perkin-Elmer Applied Biosystems, Foster City, CA, USA) following the manufacturer's instructions, and run on an ABI PRISM™ 3100 automated DNA sequencer (Perkin-Elmer Applied Biosystems, Foster City, CA, USA).

2.8 Phylogenetic Analysis

The obtained sequences were manually checked and edited where necessary using MEGA 11 (Tamura, Stecher, & Kumar, 2021). The sequence generated in this study, together with 25 reference sequences of related Asteraceae species retrieved from the NCBI GenBank database (Table 1), was aligned using MAFFT (Katoh, Kuma, Toh, & Miyata, 2005). All sequences were subjected to a nucleotide BLAST search via NCBI (https://www.ncbi.nlm.nih.gov, accessed on 20 June 2025) to assess similarity with closely related taxa. MEGA v.11 was used for trimming and concatenating the multiple sequence alignment (Tamura et al., 2021). The final alignment comprised 26 sequences with 1216 aligned positions, including 61 distinct patterns, 26 parsimony-informative sites, 25 singleton sites, and 1165 constant sites. Based on the Bayesian Information Criterion (BIC) implemented in ModelFinder (Kalyaanamoorthy, Minh, Wong, Von Haeseler, & Jermiin, 2017), TPM3u+F+I was selected as the best-fit substitution model. IQ-TREE multicore version 2.2.0 (Minh et al., 2020) was used to infer the maximum-likelihood (ML) phylogenetic tree, with node support assessed using 10,000 ultrafast bootstrap replicates (Hoang, Chernomor, Von Haeseler, Minh, & Vinh, 2018) on the partitioned dataset (Chernomor, Von Haeseler, & Minh, 2016). The resulting ML tree was visualized in FigTree v.1.4.4 (http://tree.bio.ed.ac.uk/software/figtree, accessed on 20 June 2025).

Table 1. Reference plant sequences of the *rbcL* gene region retrieved from GenBank and used in the phylogenetic analysis.

Species name	NCBI Taxonomy ID	Country of origin	GenBank accession number
Embergeria grandifolia	43192	New Zealand	JQ933322
Reichardia intermedia	268088	Portugal	MN783844
Launaea cervicornis	2201912	Pakistan	MG946919
Launaea nudicaulis	43200	Pakistan	MG946892
Launaea secunda	1205754	Nepal	JQ933380
Launaea sarmentosa	381725	China	MH767500
Hieracium levicaule	651084	New Zealand	GQ120446
Hippolytia gossypina	1898838	China	KX527022
Lygodesmia aphylla	1620143	USA	KJ773664
Dubyaea hispida	996389	Nepal	JQ933313
Youngia racemifera	1205803	Nepal	JQ933524
Hieracium umbellatum	268065	Bhutan	JQ933362
Hieracium pilosella	221204	Switzerland	KF602082
Hieracium villosum	269347	Switzerland	KF602084
Sonchus oleraceus	50207	USA	EU385018
Sonchus oleraceus	50207	United Kingdom	KM360989
Sonchus oleraceus	50207	USA	MN601475
Sonchus oleraceus	50207	South Korea	OR908611
Sonchus arvensis	50192	Canada	JX848427
Sonchus arvensis	50192	USA	MN601474
Sonchus wightianus	1205783	Nepal	JQ933486
Pyrrhopappus carolinianus	231826	USA	KJ773799
Prenanthella exigua	184946	USA	MF963115
Leontodon saxatilis	122540	Portugal	HM850115
Gynura japonica	1604314	China	KX527000

3. ETHICS APPROVAL

Not applicable. This study involved the collection of wild plant material only and did not involve human participants, human data, or animal subjects.

4. RESULT

4.1 Descriptive Statistics of Morphological and Biomass Traits

Descriptive statistics for the thirty *S. oleraceus* individuals (Table 2) revealed marked phenotypic variability across vegetative, reproductive, and biomass traits. Coefficients of variation (CV) were highest for biomass-related traits: shoot fresh weight (78.9%), root fresh weight (78.0%), and shoot dry weight (71.4%), and lowest for inflorescence length, including peduncle (17.5%) and plant height (23.5%). Root length (44.81%), inflorescence count (45.9%), leaf count (36.9%), and leaf length (28.4%) showed intermediate variability, and root dry weight was also highly variable (71.1%); the CV ranking therefore separated highly variable biomass traits (CV = 71.1–78.9%) from the more constrained structural and floral traits (CV = 17.5–28.4%). Mean shoot fresh and dry weights were 12.8 ± 10.1 g and 1.96 ± 1.4 g, respectively, and mean root fresh and dry weights were 3.46 ± 2.7 g and 0.83 ± 0.59 g. The mean plant height (40.87 cm) and leaf count (15.70) indicate that the sampled plants had reached an established vegetative phase at collection, whereas the biomass traits were the most sensitive indicators of inter-individual divergence.

Table 2. Quantitative morphological traits and biomass parameters of *S. oleraceus*.

Parameter	Mean ± SD	CV%
Plant height (cm)	40.87 ± 9.6	23.5
Root length (cm)	18.97 ± 8.5	44.81
Shoot fresh weight (g)	12.8 ± 10.1	78.9
Shoot dry weight (g)	1.96 ± 1.4	71.4
Root fresh weight (g)	3.46 ± 2.7	78.0
Root dry weight (g)	0.83 ± 0.59	71.1
Leaf count	15.7 ± 5.8	36.9
Leaf length (cm)	10.93 ± 3.1	28.4
Inflorescence count	9.37 ± 4.3	45.9
Inflorescence length with peduncle (cm)	5.04 ± 0.88	17.5

Note: Values are presented as mean ± standard deviation (n = 30). CV% = (SD ÷ Mean) × 100.

4.2 Bivariate Pearson Correlation Analysis

At n = 30 and a two-tailed $\alpha = 0.05$, correlations with $|r| \geq 0.361$ were nominally significant (Table 3). Because the matrix comprised 45 simultaneous tests, Benjamini–Hochberg false-discovery-rate (FDR) correction (q = 0.05) was applied (Section 2.4): of the 20 nominally significant correlations, 15 remained significant (Supplementary Table S3), and the interpretation below is restricted to these FDR-robust associations unless stated otherwise. Eight of the 15 had raw $p < 0.001$, and the other seven had raw p between 0.002 and 0.011.

Table 3. Pearson correlation matrix (*r*) among the ten quantitative morphological and biomass traits measured (n = 30). Trait key: 1 = Shoot fresh weight; 2 = Shoot dry weight; 3 = Root fresh weight; 4 = Root dry weight; 5 = Inflorescence count; 6 = Inflorescence length; 7 = Leaf count; 8 = Leaf length; 9 = Plant height; 10 = Root length. Coefficients are shown to two decimals; the text reports three decimals for selected values.

Trait	1	2	3	4	5	6	7	8	9	10
1	1.00									
2	0.92	1.00								
3	0.60	0.46	1.00							
4	-0.03	-0.07	0.60	1.00						
5	-0.49	-0.54	0.17	0.50	1.00					
6	-0.10	-0.02	0.15	0.15	0.41	1.00				
7	0.12	0.06	0.03	0.18	0.03	0.04	1.00			
8	0.81	0.81	0.32	-0.30	-0.49	0.06	-0.20	1.00		
9	-0.38	-0.40	0.33	0.51	0.70	0.26	-0.07	-0.48	1.00	
10	-0.33	-0.36	0.27	0.42	0.63	0.24	-0.09	-0.40	0.94	1.00

Plant height and root length showed the strongest association in the matrix (r = 0.942), followed by shoot fresh and shoot dry weight (r = 0.919). Leaf length was strongly correlated with shoot fresh weight (r = 0.814) and shoot dry weight (r = 0.806), and root fresh weight was positively correlated with shoot fresh weight (r = 0.600), shoot dry weight (r = 0.462), and root dry weight (r = 0.604). Inflorescence count was negatively correlated with shoot dry weight (r = −0.537) and shoot fresh weight (r = −0.489), yet positively correlated with plant height (r = 0.701) and root length (r = 0.633). Two correlations involving root dry weight with plant height (r = 0.507) and with inflorescence count (r = 0.501) survived FDR correction, but not microhabitat adjustment (Section 4.3), and the correlation between inflorescence count and inflorescence length (r = 0.409) did not survive FDR correction; these three are not interpreted further. Leaf length was also negatively correlated with inflorescence count (r = −0.49; within-microhabitat r = −0.37, p = 0.047, marginal) and with plant height (r = −0.48), the latter not robust to microhabitat adjustment. Leaf count was weakly correlated with all other traits.

Taken together, these associations describe coordinated vertical and belowground extension (plant height–root length), proportional scaling of tissue water content with structural biomass (shoot fresh–dry weight, which makes shoot fresh weight a practical non-destructive proxy for dry biomass), and an inverse relationship between inflorescence count and shoot biomass that is consistent with the resource-allocation hypothesis.

The latter coexists with a positive association between inflorescence count and plant height, indicating that the trade-off is expressed in biomass density rather than in stature. Leaf length emerged as a dependable architectural indicator of shoot biomass, and the positive coupling of inflorescence count with both plant height and root length (each retained after FDR correction and after accounting for microhabitat clustering) indicates that taller plants with longer roots tended to carry more inflorescences even though they allocated proportionally less dry matter to non-reproductive shoot tissue. Because no log–log regression was performed, the height–root length relationship is read as strong coordinated linear growth rather than confirmed isometric scaling.

4.3 Regression Analysis and Assessment of Microhabitat Non-Independence

Five univariate ordinary least squares (OLS) regression models were fitted (Table 4). Inflorescence count significantly predicted shoot dry weight ($Y = 3.582 - 0.1732X$; $F = 11.37$, $p = 0.002$; $R^2 = 28.89\%$, adjusted $R^2 = 26.35\%$), with each additional inflorescence associated with a decrease of approximately 0.17 g in shoot dry biomass; this model explains a modest but significant share of the variance. Residual diagnostics supported the model assumptions (Shapiro–Wilk $p = 0.215$; Breusch–Pagan $p = 0.161$; two influential observations, including sample 13 with Cook's $D = 0.32$; Supplementary Table S4), and the relationship remained significant under cluster-robust standard errors ($p = 0.013$) and in a random-intercept mixed-effects model with microhabitat as the random effect ($p = 0.001$; between-microhabitat variance ≈ 0).

Table 4. Consolidated OLS linear regression models predicting structural and reproductive trait allocations in *S. oleraceus* (n = 30).

Model	Dependent Variable (Y)	Independent Variable (X)	Regression Equation	S	R^2 (%)	R^2_adj (%)	F-value	p-value
1	Shoot Dry Weight (g)	Inflorescence Count	Y = 3.582 − 0.1732X	1.2099	28.89	26.35	11.37	0.002**
2	Inflorescence Length (cm)	Inflorescence Count	Y = 4.264 + 0.08228X	0.8180	16.71	13.73	5.62	0.025*,†
3	Shoot Dry Weight (g)	Root Dry Weight (g)	Y = 2.094 − 0.1617X	1.4314	0.47	0.00	0.13	0.720^ns
4	Shoot Dry Weight (g)	Leaf Count	Y = 1.730 + 0.01463X	1.4322	0.36	0.00	0.10	0.752^ns
5	Inflorescence Count	Leaf Count	Y = 9.056 + 0.0198X	4.4505	0.07	0.00	0.02	0.891^ns

Note: ** and * indicate statistical significance at the 99% ($p \leq 0.01$) and 95% ($p \leq 0.05$) confidence thresholds, respectively; ^ns denotes non-significant relationships. S represents the standard error of the regression. † This nominally significant model (Model 2) did not survive Benjamini–Hochberg correction for multiple comparisons (Section 4.2) and showed heteroscedastic residuals (Section 4.3); it is excluded from the main interpretive narrative and reported for transparency only (see Table S4).

The model relating inflorescence length to inflorescence count ($Y = 4.264 + 0.08228X$; $F = 5.62$, $p = 0.025$; $R^2 = 16.71\%$, adjusted $R^2 = 13.73\%$; approximately +0.082 cm per additional inflorescence) was significant only nominally: it corresponds to the correlation ($r = 0.409$) that did not survive FDR correction, and its residuals were heteroscedastic (Breusch–Pagan $p = 0.033$), with four influential observations (Table S4). It is therefore reported for transparency and excluded from the interpretive narrative. The remaining models shoot dry weight on root dry weight ($F = 0.13$, $p = 0.720$; $R^2 = 0.47\%$), shoot dry weight on leaf count ($F = 0.10$, $p = 0.752$; $R^2 = 0.36\%$), and inflorescence count on leaf count ($F = 0.02$, $p = 0.891$; $R^2 = 0.07\%$) were non-significant, with negligible explained variance and adjusted $R^2 = 0.00\%$, indicating that at this developmental stage shoot biomass varied largely independently of root biomass and leaf count. Residuals departed from normality in the first two of these models (Shapiro–Wilk $p = 0.009$ and 0.004), which does not alter the conclusion of no linear association, and each null model had two influential observations (Table S4). These outcomes point to leaf area, rather than leaf count, as a more informative predictor to be tested in hierarchical models.

Because plants were sampled in balanced blocks of five from each of six microhabitats, non-independence was evaluated explicitly (Section 2.4). Microhabitat clustering was negligible (ICC ≈ 0) for shoot fresh and dry weight, root fresh weight, inflorescence length, and leaf count, very low for leaf length (ICC = 0.03), moderate for root dry weight (ICC = 0.25; design effect = 1.98) and inflorescence count (ICC = 0.11), and substantial for plant height (ICC = 0.40; ANOVA $p = 0.006$) and root length (ICC = 0.44; $p = 0.003$) (Table S5a).

Treating individuals as independent observations is therefore justified for the weakly clustered traits, and the principal regression model, being driven by weakly clustered traits, was not an artifact of the nested design. The height–root length correlation nevertheless remained strong within microhabitats (partial $r = 0.90$, $p < 0.001$) and between microhabitat means ($r = 0.985$, $n = 6$), and it was robust with or without the three influential observations (samples 4, 15, and 24; Cook's distance > 4/n; Fig. S1). Of the 15 FDR-significant correlations, 12 remained significant after within-microhabitat adjustment (Table S5b) for example, within-site $r = 0.93$ for shoot fresh–dry weight, 0.85 and 0.80 for leaf length with shoot fresh and dry weight, 0.58 and 0.48 for inflorescence count with plant height and root length, and −0.50 and −0.45 for inflorescence count with shoot dry and fresh weight including all those central to the interpretation in Section 5.3. The three that did not show plant height with root dry weight (within-site $r = 0.19$, $p = 0.321$), inflorescence count with root dry weight ($r = 0.30$, $p = 0.110$), and plant height with leaf length ($r = −0.32$, $p = 0.084$) are attributed to covariation among microhabitats rather than individual-level coupling and are not interpreted further.

4.4 Morphological Voucher Documentation and Confirmation

The comparative morphological survey of fresh and pressed voucher material (Fig. 1A–H) confirmed that the diagnostic vegetative and reproductive traits of the studied accession are fully consistent with the taxonomic circumscription of *S. oleraceus* L. (Asteraceae, tribe Cichorieae) and with the descriptions of Puri et al. (2018) and Sadeq and Aliwy (2019). Plants were erect, sparsely branched annual herbs arising from a short, fleshy taproot (Fig. 1A), a habit typical of ruderal Cichorieae of disturbed, nutrient-rich substrates (Hutchinson et al., 1984; Ollivier, Gauthier, et al., 2020). At the pre-bolting stage the leaves formed a prostrate basal rosette (Fig. 1B, C), documented in situ on reddish loamy soil and as a pressed voucher against a linear scale; its runcinate-pinnatifid lamina, together with achene sculpture, is one of the two characters classically used to separate *S. oleraceus* from the morphologically close *S. asper* (L.) Hill (Boulos, 1973; Hutchinson et al., 1984; Mejías & Andrés, 2004; Ollivier, Gauthier, et al., 2020).

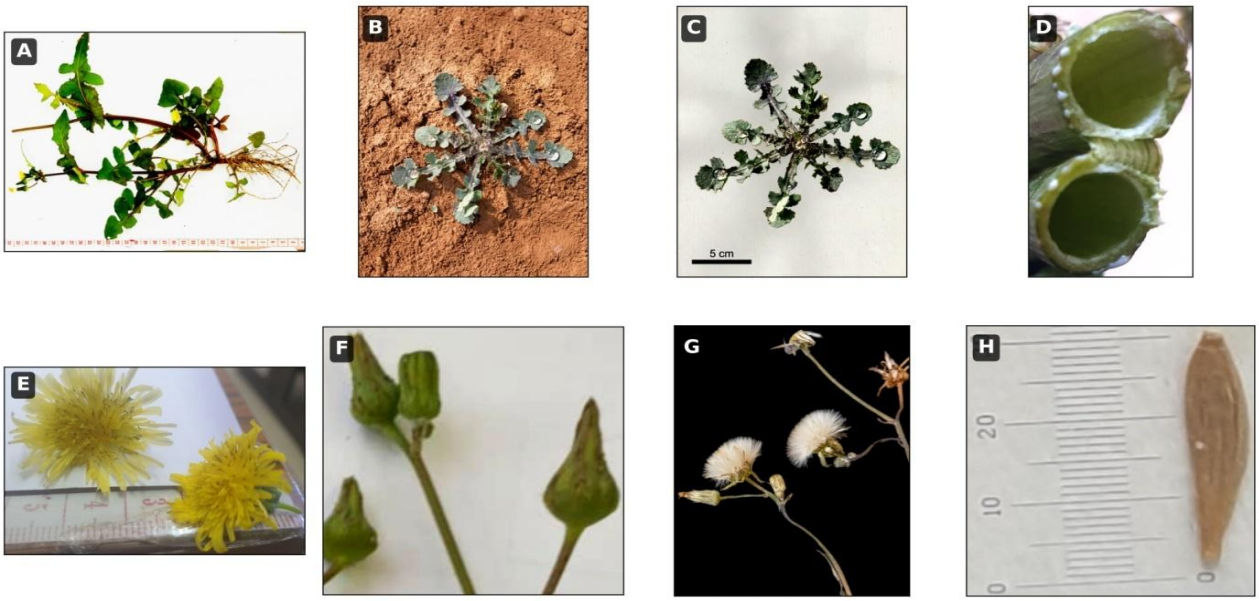


Fig. 1. Vegetative and reproductive morphology of *S. oleraceus* L. (A) Whole-plant habit, showing the erect, sparsely branched shoot arising from a short taproot, photographed against a linear scale. (B) Basal leaf rosette in situ on the native reddish loamy substrate. (C) Pressed voucher of the basal rosette photographed against a linear scale (5 cm). (D) Transverse sections of paired fistular, longitudinally ridged stem internodes, showing beads of milky latex exuded from the cut surface. (E) Capitula at full anthesis, showing numerous ligulate florets subtended by a glabrous, imbricate involucre, photographed against a linear scale. (F) Post-anthetic capitula, showing the involucral bracts closed tightly around the developing achenes following corolla senescence and before pappus exsertion. (G) Post-anthetic capitula with the involucre re-opened, exposing the exserted, globose pappus of fine white capillary bristles that mediates anemochorous dispersal. (H) Isolated mature achene (cypsela), showing the longitudinally ribbed, transversely wrinkled pericarp, photographed against a microscope-slide micrometer scale (0.1 mm graduations). Transverse sections of the flowering stem (Fig. 1D) exposed the characteristic fistular, longitudinally ridged internode, with beads of milky latex exuded on cutting, a feature repeatedly reported for the genus (Hutchinson et al., 1984).

At anthesis, the capitula (Fig. 1E) were homogamous and exclusively ligulate, bearing more than 100 bright-yellow florets per capitulum subtended by a glabrous, imbricate involucre, in close agreement with published descriptions (Tadesse, 2004).

After corolla senescence, the capitula closed around the developing fruits (Fig. 1F) and later re-opened to expose a globose pappus of fine white capillary bristles (Fig. 1G), the structure underlying the wind dispersal widely regarded as a principal contributor to the weediness of the species (Hutchinson et al., 1984; Manalil, Ali, & Chauhan, 2018; Widderick, Walker, Sindel, & Bell, 2010). The mature achene (Fig. 1H) was narrowly obovoid, dorsiventrally compressed, light brown, and beakless, with longitudinal ribs alternating with fine transverse wrinkles and a length in the 2.5–4.0 mm range among the most reliable single characters for identifying *S. oleraceus* within *Sonchus* (Hutchinson et al., 1984; Mejías & Andrés, 2004; Ollivier, Gauthier, et al., 2020). The voucher characters were recorded on the same population that supplied the quantitative measurements and the pooled molecular sample (Section 2.5). Together, these attributes corroborate earlier taxonomic and cytogenetic accounts of *S. oleraceus* as a putative amphidiploid derivative of *S. asper* × *S. tenerrimus* L. (Boulos, 1973; Cho et al., 2019; Mejías & Andrés, 2004) and provide a voucher-based morphological framework for the quantitative analyses above.

4.5 Molecular Confirmation and Phylogenetic Placement

PCR amplification with the *rbcL*-BF/*rbcL*-724R primer pair yielded amplicons of 700–750 bp, matching the expected size for a partial *rbcL* region, and the identification of the sampled specimen as *S. oleraceus* was confirmed at the species level by phylogenetic analysis of this region together with the GenBank reference sequences (Table 1). Preliminary BLAST searches indicated close affinity with deposited *S. oleraceus* sequences, and the maximum-likelihood tree (Fig. 2; reference sequences in Table 1) placed the accession deeply within the clade of the four reference *S. oleraceus* sequences (bootstrap = 98%), sister to *S. arvensis* (bootstrap = 96%). The final alignment comprised 26 sequences and 1,216 aligned positions (26 parsimony-informative sites; Section 2.8), and TPM3u+F+I was the best-fit substitution model. Across the reference dataset, which spanned related Asteraceae genera (e.g., *Launaea*, *Hieracium*, *Youngia*, *Reichardia*, and *Leontodon*), rbcL provided a highly resolved and strongly supported separation of *S. oleraceus* from other species and related taxa, and *Sonchus* was clearly distinguished from all other genera.

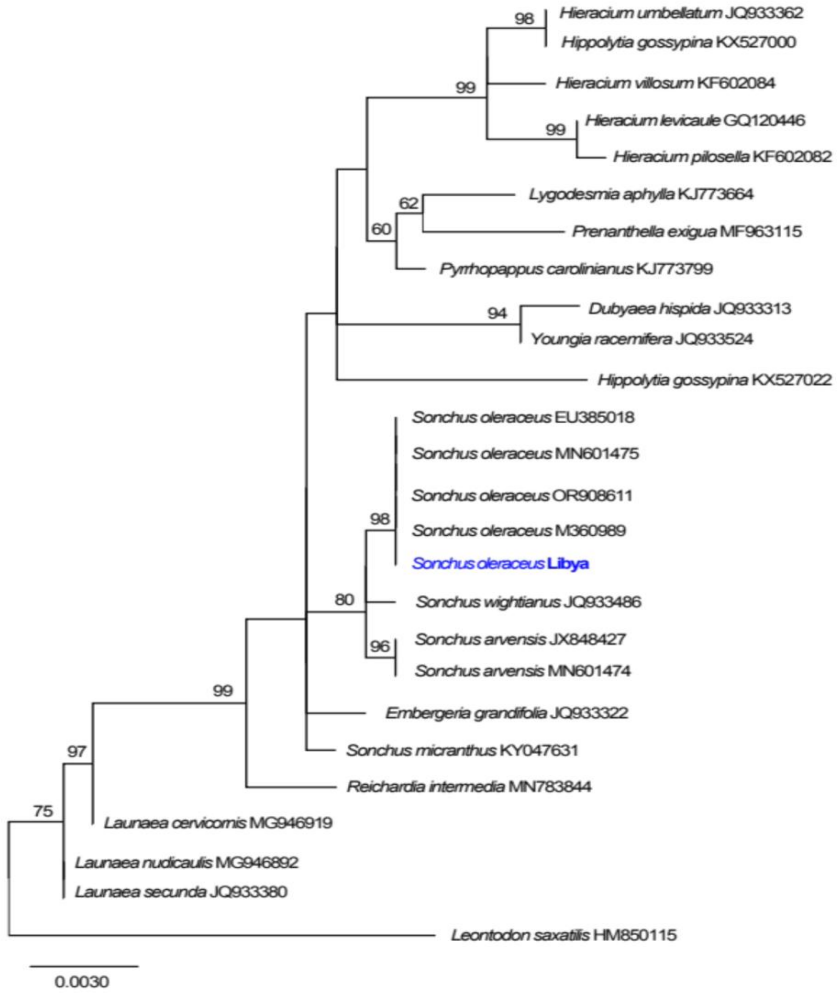


Fig. 2. Maximum likelihood tree derived from phylogenetic inference analyses of *rbcL* sequences, with indication of the position of the analyzed *S. oleraceus* sample (highlighted in blue). Bootstrap support (BS) values (≥ 50%) are shown above branches. The tree was rooted using the outgroup taxon *Leontodon saxatilis* HM850115.

The accession was a composite sample from the 30 individuals measured morphologically, so the molecular result independently corroborates the morphology-based identification of that population and illustrates the value of combining classical taxonomy with barcoding, consistent with the universality and ease of amplification that make *rbcL* a widely used plastid barcode (CBOL Plant Working Group, 2009; Hollingsworth et al., 2011). Within *Sonchus*, the accession grouped with *S. oleraceus* sequences of diverse geographic origin (United States, United Kingdom, South Korea) and with *S. wightianus*, a pattern consistent with earlier plastid and nuclear marker studies (Kim et al., 2007) and compatible with limited geographic structuring of chloroplast lineages (Cho et al., 2019). *S. asper* was absent from the dataset; its reported close relationship to *S. oleraceus*, and the proposed role of hybridization and polyploidization in the history of the group, derive from published plastome work (Cho et al., 2019) and were not tested here.

Although *rbcL* evolves more slowly than ITS or matK, it generally yields stable genus- and species-level reconstructions given adequate reference sampling (Hollingsworth et al., 2011). Not all nodes were equally well supported, echoing the known difficulty of resolving closely related *Sonchus* lineages (Kim et al., 2007), a limitation compounded here by reliance on a single locus and a single pooled accession. The analysis therefore establishes species-level identity but cannot address intraspecific diversity or hybrid origin, which would require multi-marker, multi-individual sampling (Encinas-Viso et al., 2022; Kim et al., 2020). Given the overlapping morphology of many *Sonchus* species, molecular confirmation of a representative accession adds reliability to the morphological dataset for subsequent ecological, phytochemical, and conservation work.

5. DISCUSSION

5.1 Trait Variability and Relative Stability

Trait variability followed a clear hierarchy. Biomass traits were the most variable (shoot fresh weight CV = 78.9%; root dry weight CV = 71.1%), architectural traits were intermediate (plant height CV = 23.5%; leaf count CV = 36.9%; root length CV = 44.81%), and inflorescence length was the most uniform trait (CV = 17.5%). Low variability in floral structures is consistent with theory predicting that traits governing pollinator fit are buffered against environmental noise by stabilizing selection (Armbruster, Hansen, Pélabon, Pérez-Barrales, & Maad, 2009; Herrera, 2017), although this interpretation is not tested here: single-season, single-site data cannot separate genetic from environmental sources of variation. The contrast between variable vegetative and biomass traits and a comparatively stable floral trait is commonly described as a plasticity canalization pattern in ruderal annuals exploiting heterogeneous, disturbed habitats (Matesanz, Gianoli, & Valladares, 2010), and the extreme variance in gravimetric traits (CV = 71.1–78.9%) agrees with reports that *Sonchus* dry matter production is highly sensitive to micro-topographic and moisture conditions (Chauhan, Widderick, Werth, & Cook, 2015; Hutchinson et al., 1984).

Reproductive traits were not uniformly stable, however: inflorescence count varied substantially (CV = 45.9%; 9.37 ± 4.3 per plant), although less than biomass traits. Mean plant height (40.87 ± 9.6 cm) and inflorescence count were well below the 100–150 cm and approximately 44 capitula reported for plants under favorable agricultural conditions (Ahmad, Abdallah, & Kamil, 2021; Chauhan et al., 2015; Hutchinson et al., 1984), which may reflect sampling at early anthesis around the rosette-to-bolting transition, growth under local environmental constraints, or both. The uniformity of inflorescence length (5.04 ± 0.88 cm) may likewise reflect the standardized anthesis stage of sampling, since inflorescences elongate to about 10 cm at seed maturity (Ahmad et al., 2021; Chauhan et al., 2015).

5.2 Climatic Context

Meteorological records for 2023–2025 (Supplementary Tables S1 and S2) provide a plausible environmental context for the modest vegetative attainment of the sampled plants. Cumulative January–May rainfall declined progressively, from 270.9 mm in 2023 to 177.8 mm in 2024 and 116.4 mm in 2025, corresponding to reductions of 34.4% between 2023 and 2024 and 34.5% between 2024 and 2025 (57.0% overall between 2023 and 2025). Rainfall was particularly limited during early establishment (January–February 2025: 25.3 and 33.3 mm), a period when restricted soil moisture may constrain leaf production and leaf expansion. Experimental evidence is consistent with this expectation: in *S. oleraceus* grown under three soil-moisture regimes, moderate and severe water limitation reduced total leaf area by approximately 42% and 61% and leaf number by approximately 35% and 47%, respectively, relative to well-watered plants (Peerzada, Williams, O'Donnell, & Adkins, 2021), and leaf area likewise decreased with increasing water stress in the congeneric *S. arvensis* (Rahardjo & Darwati, 2000).

February 2025 was also colder than February 2024 (minimum 5.88 vs. 7.06 °C; mean 9.19 vs. 10.58 °C), a condition generally associated with reduced carbon gain (Chaves, Flexas, & Pinheiro, 2009). In addition, the rapid warming in May (maximum 24.98 °C) under continuing moisture limitation may have favored earlier reproductive development over vegetative growth (Ramesh, Matloob, Aslam & Florentine, 2017; Chauhan, 2015), and the high variability of root length (CV = 44.81%; 18.97 ± 8.5 cm) may reflect heterogeneous moisture and nutrient availability among microsites (Freschet et al., 2021; Lynch, 2013). These observations fit this climatic context, but the links remain inferential: the data are correlational, no physiological variables (e.g., stomatal conductance or leaf water potential) were measured, sampling stage may have contributed to the observed values, and genetic and environmental sources of variation could not be separated. The climatic record is therefore offered as a plausible context rather than a demonstrated causal mechanism, to be tested through dedicated ecophysiological monitoring.

5.3 Trait Integration and Allocation Trade-Offs

Shoot fresh and dry weight were strongly coupled (r = 0.919), and the high fresh-to-dry ratio (shoot water content ≈ 85%) is typical of fast-growing, acquisitive ruderal herbs positioned toward the "fast" end of the plant economics spectrum (Reich, 2014). Intraspecific variability of this magnitude can rival interspecific variation in shaping community dynamics (Violle et al., 2012), and the capacity to establish across variable environments is a recurrent attribute of widespread weeds (Lee, 2002). Shoot fresh weight is therefore a reasonable proxy for dry matter production (Díaz et al., 2016; Poorter et al., 2012), whereas root dry weight varied independently of shoot dry weight (Section 4.3), possibly reflecting microsite heterogeneity. Root fresh weight nevertheless covaried with shoot fresh and dry weight (r = 0.600 and 0.462), pointing to integrated above- and belowground biomass accumulation (Freschet et al., 2021).

The inverse relationship between inflorescence count and shoot biomass (r = −0.489 and −0.537 for fresh and dry weight; regression R^2 = 28.89%, p = 0.002) is consistent with the resource-allocation hypothesis, under which reproductive structures compete with vegetative tissues for assimilates (Obeso, 2002; Weiner, Campbell, Pino, & Echarte, 2009). This association persisted within microhabitats and in mixed-effects models (Section 4.3), but it is correlational and does not identify the underlying mechanism; the slope (≈ −0.17 g per inflorescence) best describes this single-site sample. Inflorescence count also correlated positively with plant height (r = 0.701) and root length (r = 0.633), relationships that remained significant after FDR and microhabitat adjustment, suggesting that taller plants with longer roots tended to bear more inflorescences, in line with the recognized role of belowground traits in plant performance (Bardgett, Mommer, & De Vries, 2014; Freschet et al., 2021).

Plant height and root length were the most tightly integrated pair of traits (r = 0.942; within-microhabitat r = 0.90; between-microhabitat r = 0.985), a coordination of vertical and belowground extension that proved robust to the nested design (Díaz et al., 2016; Reich, 2014). Leaf length was strongly correlated with shoot fresh and dry weight (r = 0.814 and 0.806), consistent with leaf-economics expectations that larger leaf area supports greater carbon gain, whereas leaf count was weakly correlated with all traits and is a poor biomass predictor by comparison (Wright et al., 2004). The negative correlation of leaf length with inflorescence count (r = −0.49) indicates that larger-leaved individuals tended to bear fewer inflorescences, although this association is tentative given its marginal support after microhabitat adjustment (within-site p = 0.047).

The regression analyses reinforced this picture. The inflorescence count–shoot dry weight relationship, a trade-off previously reported in *S. oleraceus* and other annual herbs (Ollivier, Kazakou, et al., 2020), was the only robust model; shoot dry weight was unrelated to root dry weight or leaf count, and inflorescence count was unrelated to leaf count (all p > 0.7), suggesting that biomass depends more on leaf area than on leaf number, as reported for nutrient effects on leaf area and biomass (Carrascosa-Robles, Pascual, Ros, Petropoulos, & Alguacil, 2022). The nominal association between inflorescence count and inflorescence length (R^2 = 16.71%, p = 0.025) did not survive FDR correction and is not interpreted. The generally low R^2 values indicate that much trait variability remains unexplained, pointing to unmeasured genetic, edaphic, or physiological factors and to the need for studies integrating morphological, physiological, and ecological variables.

6. CONCLUSION

This study provides an integrated morphological–molecular characterization of wild *Sonchus oleraceus* L. from the Omar Al-Mukhtar University campus, Al-Bayda (Al-Jabal Al-Akhdar region), Libya. Voucher-based morphology and *rbcL* barcoding were concordant: the accession fell within a strongly supported *S. oleraceus* clade (bootstrap = 98%), sister to *S. arvensis* (bootstrap = 96%), and the sequence constitutes a first *rbcL* reference for the species from Libya, where North African records in GenBank and BOLD Systems remain near-absent.

Vegetative and biomass traits were highly variable (CV up to 78.9%), whereas inflorescence length was comparatively uniform (CV = 17.5%). Plant height and root length were tightly associated ($r = 0.942$), and inflorescence count was inversely related to shoot dry weight ($R^2 = 28.89\%$, $p = 0.002$), a pattern consistent with resource allocation between reproduction and vegetative biomass that remained robust to FDR correction and microhabitat clustering.

Meteorological records for 2023–2025 show declining rainfall and offer a plausible context for the modest vegetative development observed, although this link remains an inference rather than a demonstrated cause.

Limitations include a single-site, single-season sample of 30 individuals, correlational inference, and a single pooled *rbcL* accession, which confirms species identity but cannot address intraspecific genetic diversity, population structure, or hybrid origin. Future work should combine multi-site, multi-season sampling with soil-moisture monitoring and physiological measurements, adopt leaf-area-based descriptors in mixed-effects models, and extend barcoding to multiple individuals and loci (*matK*, ITS/ITS2) alongside genomic approaches, with validated Libyan sequences deposited in GenBank and BOLD Systems.

ACKNOWLEDGMENT

The authors thank the Department of Forestry, Faculty of Natural Resources and Environmental Science, Omar Al-Mukhtar University, for providing field access and laboratory facilities used in this study. The authors also thank Abdulsalam M. Agwaidar for providing the climatic data (solar radiation and meteorological records) cited in this study.

FUNDING

This research received no specific grant from any funding agency in the public, commercial, or not-for-profit sectors.

CONFLICTS OF INTEREST

The authors declare that they have no known competing financial interests or personal relationships that could have appeared to influence the work reported in this paper.

DATA AVAILABILITY STATEMENT

The rbcL sequence generated in this study has been deposited and is available upon request from the corresponding author. The raw morphometric and biomass dataset, together with the R/Python scripts used for the statistical analyses reported in Sections 2.4, 3.24.2, and 3.34.3, are available from the corresponding author upon reasonable request.

AUTHOR CONTRIBUTIONS

Conceptualization and study design: Z.K.I.; field sampling and morphological data collection: L.S.E.-S.; molecular laboratory work and data curation: A.M.I.; statistical analysis: Z.K.I. and L.S.E.-S.; writing original draft preparation: L.S.E.-S.; writing review and editing: Z.K.I. and A.M.I.; supervision: Z.K.I. All authors have read and agreed to the published version of the manuscript, and take public responsibility for its content.

SUPPLEMENTARY MATERIALS

The following supplementary figures and tables provide the full statistical detail underlying the multiple-comparison correction, regression diagnostics, and microhabitat-clustering assessment described in Sections 2.4, 3.24.2, and 3.34.3.

Table S1. Monthly distribution of rainfall (mm) recorded in the study area during 2023–2025.

Month	2023 (mm)	2024 (mm)	2025 (mm)
1	102.3	104.6	25.3
2	108.7	58.6	33.3
3	30.0	6.9	27.6
4	12.6	0.7	17.1
5	17.3	7.0	13.1
6	2.5	0.6	0.6
7	0.0	0.0	0.1
8	0.4	6.5	1.4
9	74.1	4.5	1.7
10	13.0	2.8	22.7
11	17.5	27.5	49.8
12	61.7	116.7	94.2

Table S2. Monthly variations in temperature (maximum, minimum, and mean) and relative humidity during 2024–2025.

Year	Month	Max. Temperature (℃)	Min. Temperature (℃)	Mean Temperature (℃)	Relative Humidity (%)
	2	14.10	7.06	10.58	74.72
	3	17.01	8.32	12.66	71.37
	4	22.68	11.67	17.18	54.93
	5	25.82	14.94	20.38	52.45
	6	31.36	19.60	25.48	44.63
	7	29.69	19.21	24.45	64.39
	8	30.18	19.30	24.74	65.06
	9	30.28	17.90	24.09	70.50
	10	24.45	14.73	19.59	68.45
	11	18.16	11.04	14.60	74.73
	12	14.43	8.02	11.22	80.16
	2	12.49	5.88	9.19	76.71
	3	19.10	10.09	14.60	55.81
	4	18.79	9.82	14.31	69.66
	5	24.98	14.84	19.91	51.39
	6	26.77	16.55	21.66	56.93
	7	29.24	18.88	24.06	59.84
	8	28.57	18.63	23.60	68.19
	9	26.59	17.11	21.85	70.80
	10	22.73	13.80	18.26	69.39
	11	18.83	11.79	15.31	69.23
	12	14.72	8.10	11.41	79.55
2024	1	13.68	7.68	10.68	77.81
2025	1	14.88	8.15	11.51	75.68

Table S3. Exact two-tailed p-values and Benjamini–Hochberg (FDR, q = 0.05) correction results for all 45 pairwise Pearson correlations among the ten quantitative traits (n = 30, df = 28).

Trait A	Trait B	r	p (raw)	Significant after FDR (q=0.05)
Root length	Plant height	0.94	<0.001	Yes
Shoot dry weight	Shoot fresh weight	0.92	<0.001	Yes
Leaf length	Shoot fresh weight	0.81	<0.001	Yes
Leaf length	Shoot dry weight	0.81	<0.001	Yes
Plant height	Inflorescence count	0.70	<0.001	Yes
Root length	Inflorescence count	0.63	<0.001	Yes
Root fresh weight	Shoot fresh weight	0.60	<0.001	Yes
Root dry weight	Root fresh weight	0.60	<0.001	Yes
Inflorescence count	Shoot dry weight	-0.54	0.002	Yes
Plant height	Root dry weight	0.51	0.004	Yes
Inflorescence count	Root dry weight	0.50	0.005	Yes
Inflorescence count	Shoot fresh weight	-0.49	0.006	yes
Leaf length	Inflorescence count	-0.49	0.006	yes
Plant height	Leaf length	-0.48	0.007	yes
Root fresh weight	Shoot dry weight	0.46	0.011	yes
Root length	Root dry weight	0.42	0.021	no
Inflorescence length	Inflorescence count	0.41	0.024	no
Plant height	Shoot dry weight	-0.40	0.029	no
Root length	Leaf length	-0.40	0.029	no
Plant height	Shoot fresh weight	-0.38	0.038	no
Root length	Shoot dry weight	-0.36	0.051	no
Plant height	Root fresh weight	0.33	0.075	no
Root length	Shoot fresh weight	-0.33	0.075	no
Leaf length	Root fresh weight	0.32	0.085	no
Leaf length	Root dry weight	-0.30	0.107	no
Root length	Root fresh weight	0.27	0.149	no
Plant height	Inflorescence length	0.26	0.165	no
Root length	Inflorescence length	0.24	0.201	no
Leaf length	Leaf count	-0.20	0.289	no
Leaf count	Root dry weight	0.18	0.341	no
Inflorescence count	Root fresh weight	0.17	0.369	no
Inflorescence length	Root fresh weight	0.15	0.429	no
Inflorescence length	Root dry weight	0.15	0.429	no
Leaf count	Shoot fresh weight	0.12	0.528	no
Inflorescence length	Shoot fresh weight	-0.10	0.599	no
Root length	Leaf count	-0.09	0.636	no
Root dry weight	Shoot dry weight	-0.07	0.713	no
Plant height	Leaf count	-0.07	0.713	no
Leaf count	Shoot dry weight	0.06	0.753	no
Leaf length	Inflorescence length	0.06	0.753	no
Leaf count	Inflorescence length	0.04	0.834	no
Root dry weight	Shoot fresh weight	-0.03	0.875	no
Leaf count	Root fresh weight	0.03	0.875	no
Leaf count	Inflorescence count	0.03	0.875	no
Inflorescence length	Shoot dry weight	-0.02	0.916	no

Table S4. Residual diagnostics for the five OLS regression models reported in Table 4 (Shapiro–Wilk test for normality; Breusch Pagan test for homoscedasticity; Cook's distance for influential observations, threshold 4/n = 0.133).

Model	R^2 / p	Shapiro–Wilk	Breusch–Pagan	Influential points
Model 1: Shoot dry wt ~ Inflorescence count	R^2=28.89%, p=0.002	p=0.215 (OK)	p=0.161 (OK)	2 (sample 13, D=0.32)
Model 2: Inflorescence length ~ Inflorescence count	R^2=16.71%, p=0.025	p=0.369 (OK)	p=0.033 (violated)	4 (samples 29, 14, 17, +1)
Model 3: Shoot dry wt ~ Root dry wt	R^2=0.47%, p=0.720	p=0.009 (violated)	p=0.270 (OK)	2 (samples 3, 13)
Model 4: Shoot dry wt ~ Leaf count	R^2=0.36%, p=0.752	p=0.004 (violated)	p=0.772 (OK)	2 (samples 2, 13)
Model 5: Inflorescence count ~ Leaf count	R^2=0.07%, p=0.891	p=0.186 (OK)	p=0.537 (OK)	2 (samples 2, 17)

Note: *Model numbering and the R^2 and p values follow Table 4 exactly. Model 2 was significant only nominally and showed heteroscedastic residuals (Section 4.3).*

Table S5a. Intraclass correlation coefficient (ICC) attributable to microhabitat for each quantitative trait, with corresponding one-way ANOVA p-value and design effect (Deff = 1 + (m−1)×ICC, m = 5 plants per microhabitat).

Trait	ANOVA p (site effect)	ICC	Design effect (Deff)
Shoot fresh weight	0.606	0.000	1.00
Shoot dry weight	0.561	0.000	1.00
Root fresh weight	0.812	0.000	1.00
Root dry weight	0.050	0.245	1.98
Inflorescence count	0.202	0.105	1.42
Inflorescence length	0.491	0.000	1.00
Leaf count	0.426	0.005	1.02
Leaf length (mean)	0.352	0.033	1.13
Plant height	0.006	0.398	2.59
Root length	0.003	0.444	2.77

Table S5b. Within-microhabitat (partial) correlation re-analysis of the fifteen correlations that remained significant after FDR correction (Table S3), computed after residualizing both variables on microhabitat (n = 30, 6 microhabitats).

Trait A	Trait B	Raw r (pooled)	Within-site r	Within-site p	Robust to clustering?
Root length	Plant height	0.94	0.90	<0.001	Yes
Shoot dry weight	Shoot fresh weight	0.92	0.93	<0.001	Yes
Leaf length	Shoot fresh weight	0.81	0.85	<0.001	Yes
Leaf length	Shoot dry weight	0.81	0.80	<0.001	Yes
Plant height	Inflorescence count	0.70	0.58	0.001	Yes
Root length	Inflorescence count	0.63	0.48	0.007	Yes
Root fresh weight	Shoot fresh weight	0.60	0.66	<0.001	Yes
Root dry weight	Root fresh weight	0.60	0.64	<0.001	Yes
Inflorescence count	Shoot dry weight	-0.54	-0.50	0.004	Yes
Plant height	Root dry weight	0.51	0.19	0.321	No
Inflorescence count	Root dry weight	0.50	0.30	0.110	No
Inflorescence count	Shoot fresh weight	-0.49	-0.45	0.012	Yes
Leaf length	Inflorescence count	-0.49	-0.37	0.047	Yes (marginal)
Plant height	Leaf length	-0.48	-0.32	0.084	No
Root fresh weight	Shoot dry weight	0.46	0.54	0.002	Yes

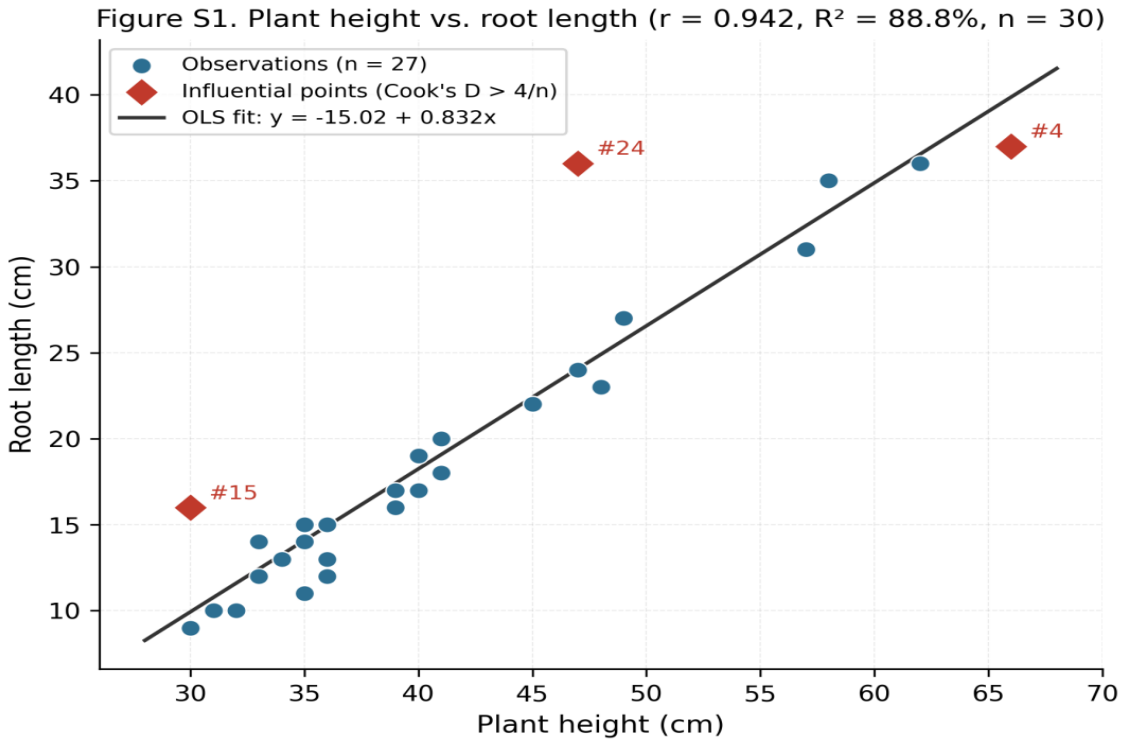


Fig. S1. Plant height vs. root length (r = 0.942, R² = 88.8%, n = 30), with an ordinary least squares regression line and influential observations (Cook's distance > 4/n) flagged in red.

7. REFERENCES

Abd El-Ghani, M., & Al Borki, A. E. N. (2024). How elevation and soil properties affect plant distribution patterns and species diversity in the Mediterranean mountain ecosystem of Al-Jabal Al-Akhdar, Libya. Journal of Mountain Science, 21, 3683–3701. https://doi.org/10.1007/s11629-024-9060-7

Ahmad, F., Abdallah, E. T., & Kamil, M. (2021). Scientific studies on aerial parts of *S. oleraceus* Linn. Arabian Journal of Medicinal & Aromatic Plants, 7, 196–214.

Alshehri, M. A., Aziz, A. T., Alzahrani, O., Alasmari, A., Ibrahim, S., Osman, G., et al. (2019). DNA-barcoding and species identification for some Saudi Arabia seaweeds using rbcL gene. Journal of Pure and Applied Microbiology, 13, 2035–2043.

Al-Traboulsi, M., & Alaib, M. A. (2021). A survey of medicinal plants of Wadi Al-Kouf in Al-Jabal Al-Akhdar, Libya. Natura Croatica, 30, 389–404. https://doi.org/10.20302/NC.2021.30.25

Armbruster, W. S., Hansen, T. F., Pélabon, C., Pérez-Barrales, R., & Maad, J. (2009). The adaptive accuracy of flowers: Measurement and microevolutionary patterns. Annals of Botany, 103, 1529–1545.

Bardgett, R. D., Mommer, L., & De Vries, F. T. (2014). Going underground: Root traits as drivers of ecosystem processes. Trends in Ecology & Evolution, 29, 692–699.

Botella, M. Á., Hellín, P., Hernández, V., Dabauza, M., Robledo, A., Sánchez, A., et al. (2024). Chemical composition of wild collected and cultivated edible plants (*S. oleraceus* L. and *Sonchus tenerrimus* L.). Plants, 13, 269.

Boulos, L. (1973). Révision systématique du genre *Sonchus* L. s.l. IV. Sous-genre 1. *Sonchus*. Botaniska Notiser, 126, 155–196.

Boulos, L. (2000). Flora of Egypt: Vol. 2. Geraniaceae–Boraginaceae. Cairo, Egypt: Al Hadara Publishing.

Carrascosa-Robles, Á., Pascual, J. A., Ros, M., Petropoulos, S. A., & Alguacil, M. M. (2022). The effect of fertilization regime on growth parameters of *S. oleraceus* L. Agronomy, 12, 2410. https://doi.org/10.3390/agronomy12102410

CBOL Plant Working Group. (2009). A DNA barcode for land plants. Proceedings of the National Academy of Sciences of the United States of America, 106, 12794–12797. https://doi.org/10.1073/pnas.0905845106

Chauhan, B. S., Widderick, M., Werth, J., & Cook, T. (2015). Common sowthistle (*Sonchus oleraceus* L.): Ecology and management. Brisbane, Australia: Department of Agriculture and Fisheries, Queensland Government.

Chaves, M. M., Flexas, J., & Pinheiro, C. (2009). Photosynthesis under drought and salt stress: Regulation mechanisms from whole plant to cell. Annals of Botany, 103, 551–560.

Chernomor, O., Von Haeseler, A., & Minh, B. Q. (2016). Terrace aware data structure for phylogenomic inference from supermatrices. Systematic Biology, 65, 997–1008.

Cho, M. S., Kim, J. H., Kim, C. S., Mejías, J. A., & Kim, S. C. (2019). Sow thistle chloroplast genomes: Insights into the plastome evolution and relationship of two weedy species, *Sonchus asper* and *S. oleraceus* (Asteraceae). Genes, 10, 881. https://doi.org/10.3390/genes10110881

de Paula Filho, G. X., Barreira, T. F., & Pinheiro-Sant'Ana, H. M. (2022). Chemical composition and nutritional value of three *Sonchus* species. International Journal of Food Science, 2022, 4181656.

Díaz, S., Kattge, J., Cornelissen, J. H. C., Wright, I. J., Lavorel, S., Dray, S., et al. (2016). The global spectrum of plant form and function. Nature, 529, 167–171. https://doi.org/10.1038/nature16489

Doyle, J. J., & Doyle, J. L. (1987). A rapid DNA isolation procedure for small quantities of fresh leaf tissue. Phytochemical Bulletin, 19, 11–15.

Encinas-Viso, F., Morin, L., Raghu, S., & Broadhurst, L. M. (2022). Population genomics reveal multiple introductions and admixture of *S. oleraceus* in Australia. Diversity and Distributions, 28, 1951–1965.

Freschet, G. T., Roumet, C., Comas, L. H., Weemstra, M., Bengough, A. G., Rewald, B., et al. (2021). Root traits as drivers of plant and ecosystem functioning: Current understanding, pitfalls and future research needs. New Phytologist, 232, 1123–1158. https://doi.org/10.1111/nph.17072

Guil-Guerrero, J. L., Giménez-Giménez, A., Rodríguez-García, I., & Torija-Isasa, M. E. (1998). Nutritional composition of *Sonchus* species (*S. asper* L, *S. oleraceus* L and *S. tenerrimus* L). Journal of the Science of Food and Agriculture, 76, 628–632.

Hebert, P. D. N., Cywinska, A., Ball, S. L., & deWaard, J. R. (2003). Biological identifications through DNA barcodes. Proceedings of the Royal Society B: Biological Sciences, 270, 313–321. https://doi.org/10.1098/rspb.2002.2218

Herrera, C. M. (2017). The ecology of subindividual variability in plants: Patterns, processes, and prospects. Web Ecology, 17, 51–64.

Hoang, D. T., Chernomor, O., Von Haeseler, A., Minh, B. Q., & Vinh, L. S. (2018). UFBoot2: Improving the ultrafast bootstrap approximation. Molecular Biology and Evolution, 35, 518–522.

Hollingsworth, P. M., Graham, S. W., & Little, D. P. (2011). Choosing and using a plant DNA barcode. PLoS ONE, 6, e19254. https://doi.org/10.1371/journal.pone.0019254

Hutchinson, I., Colosi, J., & Lewin, R. A. (1984). The biology of Canadian weeds. 63. *Sonchus asper* (L.) Hill and *S. oleraceus* L. Canadian Journal of Plant Science, 64, 731–744.

Kalyaanamoorthy, S., Minh, B. Q., Wong, T. K. F., Von Haeseler, A., & Jermiin, L. S. (2017). ModelFinder: Fast model selection for accurate phylogenetic estimates. Nature Methods, 14, 587–589. https://doi.org/10.1038/nmeth.4285

Katoh, K., Kuma, K., Toh, H., & Miyata, T. (2005). MAFFT version 5: Improvement in accuracy of multiple sequence alignment. Nucleic Acids Research, 33, 511–518. https://doi.org/10.1093/nar/gki198

Kaundal, S. P., Sharma, A., & Kulshrestha, S. (2021). Analysis of phytochemical constituents, anti-microbial activity and molecular characterization of medicinal weed *S. oleraceus* L. using RAPD marker. International Journal of Pharmaceutical Sciences and Research, 12, 6453–6463. https://doi.org/10.13040/IJPSR.0975-8232.12(12).6453-63

Kim, S. C., Lee, C., & Mejías, J. A. (2007). Phylogenetic analysis of chloroplast DNA matK gene and ITS of nrDNA sequences reveals polyphyly of the genus *Sonchus* and new relationships among the subtribe Sonchinae (Asteraceae: Cichorieae). Molecular Phylogenetics and Evolution, 44, 578–597. https://doi.org/10.1016/j.ympev.2007.03.014

Kim, S. H., Kim, H. B., Cho, M. S., Kim, C. S., & Kim, S. C. (2020). Development and characterization of 17 microsatellite markers for *S. oleraceus*. Applications in Plant Sciences, 8, e11329. https://doi.org/10.1002/aps3.11329

Lee, C. E. (2002). Evolutionary genetics of invasive species. Trends in Ecology & Evolution, 17(8), 386–391. https://doi.org/10.1016/S0169-5347(02)02554-5

Lynch, J. P. (2013). Steep, cheap and deep: An ideotype to optimize water and N acquisition by maize root systems. Annals of Botany, 112(2), 347–357. https://doi.org/10.1093/aob/mcs293

Maestre, F. T., Quero, J. L., Gotelli, N. J., Escudero, A., Ochoa, V., Delgado-Baquerizo, M., García-Gómez, M., Bowker, M. A., Soliveres, S., Escolar, C., García-Palacios, P., Berdugo, M., Valencia, E., Gozalo, B., Gallardo, A., Aguilera, L., Arredondo, T., Blones, J., Boeken, B., ... Zaady, E. (2012). Plant species richness and ecosystem multifunctionality in global drylands. Science, 335(6065), 214–218. https://doi.org/10.1126/science.1215442

Manalil, S., Ali, H. H., & Chauhan, B. S. (2018). Germination ecology of *S. oleraceus* L. in the northern region of Australia. Crop and Pasture Science, 69(9), 926–932. https://doi.org/10.1071/CP18059

Mandel, J. R., Dikow, R. B., Siniscalchi, C. M., Thapa, R., Watson, L. E., & Funk, V. A. (2019). A fully resolved backbone phylogeny reveals numerous dispersals and explosive diversifications throughout the history of Asteraceae. Proceedings of the National Academy of Sciences of the United States of America, 116(28), 14083–14088. https://doi.org/10.1073/pnas.1903871116

Matesanz, S., Gianoli, E., & Valladares, F. (2010). Global change and the evolution of phenotypic plasticity in plants. Annals of the New York Academy of Sciences, 1206, 35–55. https://doi.org/10.1111/j.1749-6632.2010.05704.x

Mejías, J. A., & Andrés, C. (2004). Karyological studies in Iberian *Sonchus* (Asteraceae: Lactuceae): *S. oleraceus*, *S. microcephalus* and *S. asper* and a general discussion. Folia Geobotanica, 39, 275–291.

Minh, B. Q., Schmidt, H. A., Chernomor, O., Schrempf, D., Woodhams, M. D., Von Haeseler, A., et al. (2020). IQ-TREE 2: New models and efficient methods for phylogenetic inference in the genomic era. Molecular Biology and Evolution, 37(5), 1530–1534. https://doi.org/10.1093/molbev/msaa015

National Aeronautics and Space Administration. (n.d.). Prediction of Worldwide Energy Resources (POWER) data access viewer. Retrieved January 23, 2026, from https://power.larc.nasa.gov/data-access-viewer/

Nithaniyal, S., Asir, B., & Sarkar, K. (2025). Recovery of DNA signatures from historical herbarium specimens using chloroplast and nuclear barcodes. Ecological Genetics and Genomics, 35, 100268. https://doi.org/10.1016/j.egg.2025.100356

Obeso, J. R. (2002). The costs of reproduction in plants. New Phytologist, 155, 321–348. https://doi.org/10.1046/j.1469-8137.2002.00477.x

Ollivier, M., Gauthier, P., Lesieur, V., Thomann, T., Jourdan, M., Bon, M. C., et al. (2020). Using karyotyping and achene morphology to accurately identify *S. oleraceus* (Asteraceae) in the context of its biological control [Preprint]. bioRxiv. https://doi.org/10.1101/2020.02.26.965863

Ollivier, M., Kazakou, E., Corbin, M., Sartori, K., Gooden, B., Lesieur, V., et al. (2020). Trait differentiation between native and introduced populations of *S. oleraceus* L. (Asteraceae). NeoBiota, 55, 85–115. https://doi.org/10.3897/neobiota.55.49158

Peerzada, A. M., Williams, A., O'Donnell, C., & Adkins, S. (2021). Effect of soil moisture regimes on the glyphosate sensitivity and morpho-physiological traits of windmill grass (*Chloris truncata* R.Br.), common sowthistle (*Sonchus oleraceus* L.), and flaxleaf fleabane [*Conyza bonariensis* (L.) Cronq.]. Plants, 10(11), 2345. https://doi.org/10.3390/plants10112345

Poorter, H., Niklas, K. J., Reich, P. B., Oleksyn, J., Poot, P., & Mommer, L. (2012). Biomass allocation to leaves, stems and roots: Meta-analyses of interspecific variation and environmental control. New Phytologist, 193, 30–50. https://doi.org/10.1111/j.1469-8137.2011.03952.x

Puri, A. V., Khandagale, P. D., & Ansari, Y. N. (2018). A review on ethnomedical, pharmacological and phytochemical aspects of *Sonchus oleraceus* Linn. (Asteraceae). *International Journal of Pharmacy and Biological Sciences*, *8*(3), 1–9.

Rahardjo, M., & Darwati, I. (2000). Pengaruh cekaman air terhadap produksi dan mutu simplisia tempuyung (*Sonchus arvensis* L.). Jurnal Penelitian Tanaman Industri, 6(3).

Ramesh, K., Matloob, A., Aslam, F., & Florentine, S. (2017). Weeds in a changing climate: Vulnerabilities, consequences, and implications for future weed management. *Frontiers in Plant Science*, *8*, Article 95. https://doi.org/10.3389/fpls.2017.00095

Reich, P. B. (2014). The world-wide 'fast–slow' plant economics spectrum: A traits manifesto. Journal of Ecology, 102, 275–301. https://doi.org/10.1111/1365-2745.12211

Ruiz-Rocamora, A., Obón, C., Ríos, S., Alcaraz, F., & Rivera, D. (2025). *Sonchus* species of the Mediterranean region: From wild food to horticultural innovation—Exploring taxonomy, cultivation, and health benefits. Horticulturae, 11, 893. https://doi.org/10.3390/horticulturae11080893

Sadeq, Z. G., & Aliwy, S. A. (2019). Micro-morphology study of pollen grains and cypsela of seven selected species belonging to Asteraceae family in Al-Jadriya campus. Iraqi Journal of Agricultural Sciences, 50(4), 1138–1152. https://doi.org/10.36103/ijas.v50i4.758

Tadesse, M. (2004). *Sonchus*. In I. Hedberg, I. Friis, & S. Edwards (Eds.), Flora of Ethiopia and Eritrea: Vol. 4(2) (pp. 65–70). Addis Ababa, Ethiopia: Addis Ababa University; Uppsala, Sweden: Uppsala University.

Tamura, K., Stecher, G., & Kumar, S. (2021). MEGA11: Molecular evolutionary genetics analysis version 11. Molecular Biology and Evolution, 38(7), 3022–3027. https://doi.org/10.1093/molbev/msab120

Violle, C., Enquist, B. J., McGill, B. J., Jiang, L., Albert, C. H., Hulshof, C., et al. (2012). The return of the variance: Intraspecific variability in community ecology. Trends in Ecology & Evolution, 27(4), 244–252. https://doi.org/10.1016/j.tree.2011.11.014

Wattoo, J. I., Saleem, M. Z., Shahzad, M. S., Arif, A., Hameed, A., & Saleem, M. A. (2016). DNA barcoding: Amplification and sequence analysis of rbcL and matK genome regions in three divergent plant species. Advances in Life Sciences, 4(1), 3–7.

Weiner, J., Campbell, L. G., Pino, J., & Echarte, L. (2009). The allometry of reproduction within plant populations. Journal of Ecology, 97, 1220–1233. https://doi.org/10.1111/j.1365-2745.2009.01559.x

Widderick, M. J., Walker, S. R., Sindel, B. M., & Bell, K. L. (2010). Germination, emergence, and persistence of *S. oleraceus*, a major crop weed in subtropical Australia. Weed Biology and Management, 10, 102–112.

Wright, I. J., Reich, P. B., Westoby, M., Ackerly, D. D., Baruch, Z., Bongers, F., et al. (2004). The worldwide leaf economics spectrum. Nature, 428, 821–827. https://doi.org/10.1038/nature02403